

AD-A084 983

ARMY ARMAMENT RESEARCH AND DEVELOPMENT COMMAND ABERD--ETC F/G 20/4
A PRELIMINARY INVESTIGATION OF THE SINGULAR BEHAVIOR OF FLUIDS --ETC(U)

MAR 80 P J ROACHE, C K ZOLTANI

ARBRL-TR-02226

UNCLASSIFIED

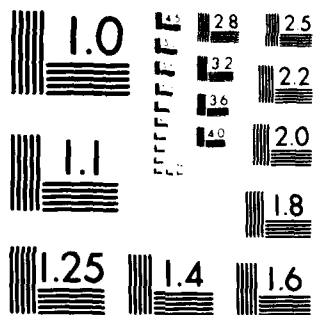
SBIE -AD-E430 433

NL

1-1
2
A. 00/007

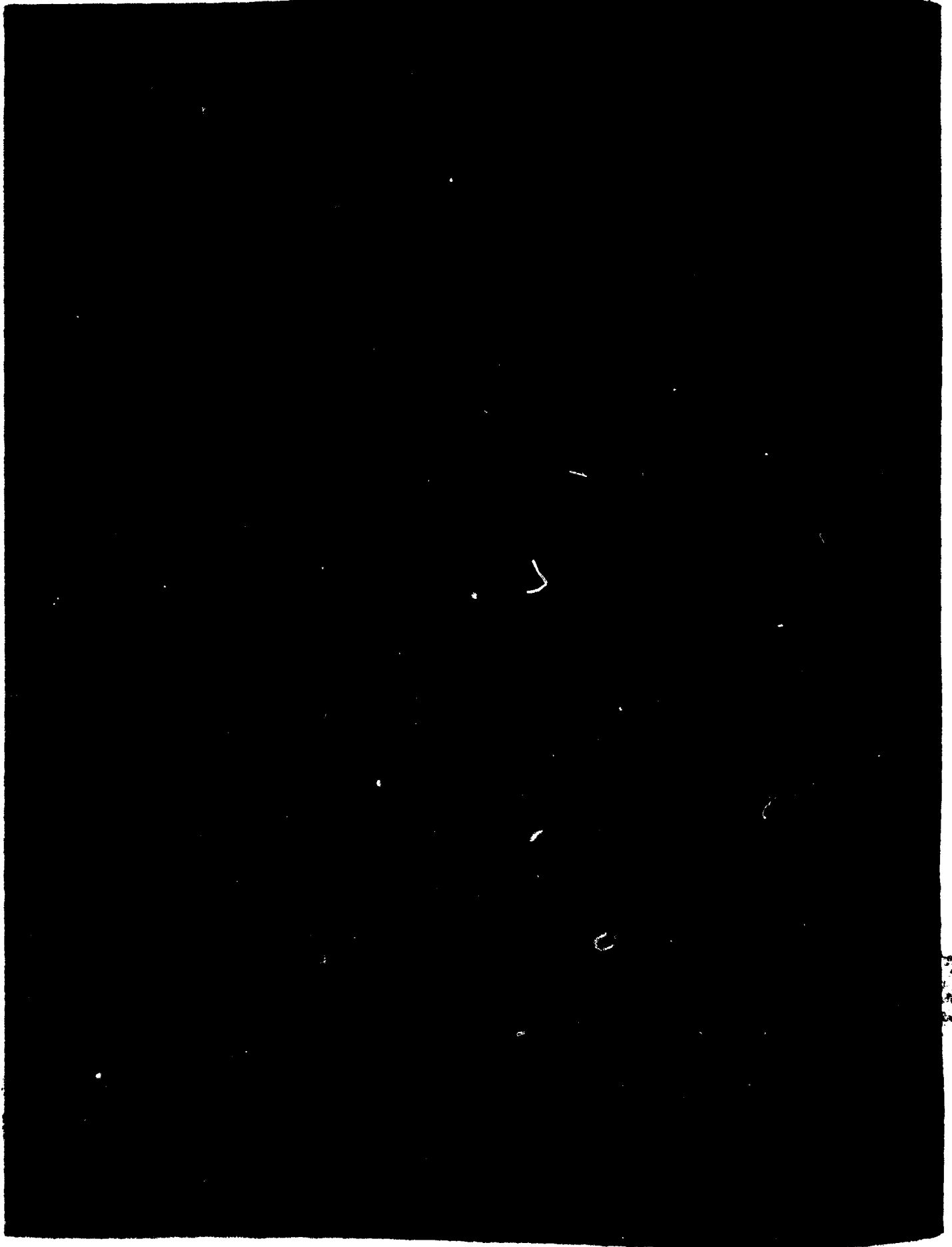


END
DATE
FILMED
7 80
DTIC



MICROCOPY RESOLUTION TEST CHART
NATIONAL BUREAU OF STANDARDS-1963-A

ADA 084983



UNCLASSIFIED

SECURITY CLASSIFICATION OF THIS PAGE (When Data Entered)

REPORT DOCUMENTATION PAGE		READ INSTRUCTIONS BEFORE COMPLETING FORM
1. REPORT NUMBER Technical Report ARBRL-TR-02226	2. GOVT ACCESSION NO. AD A084 983	3. RECIPIENT'S CATALOG NUMBER
4. TITLE (and Subtitle) A Preliminary Investigation of the Singular Behavior of Fluids Near a Sliding Corner		5. TYPE OF REPORT & PERIOD COVERED Final
7. AUTHOR(s) Patrick J. Roache Csaba K. Zoltani		6. PERFORMING ORG. REPORT NUMBER
9. PERFORMING ORGANIZATION NAME AND ADDRESS US Army Ballistic Research Laboratory ATTN: DRDAR-BLB Aberdeen Proving Ground, MD 21005		8. CONTRACT OR GRANT NUMBER(s)
11. CONTROLLING OFFICE NAME AND ADDRESS US Army Armament Research & Development Command Ballistic Research Laboratory ATTN: DRDAR-BL, APG, MD 21005		10. PROGRAM ELEMENT, PROJECT, TASK AREA & WORK UNIT NUMBERS RDT&E 1L161102AH43 DAAG29-76-C-0100
14. MONITORING AGENCY NAME & ADDRESS (if different from Controlling Office)		12. REPORT DATE MARCH 1980
		13. NUMBER OF PAGES 20
		15. SECURITY CLASS. (of this report) Unclassified
16. DISTRIBUTION STATEMENT (of this Report) Approved for public release; distribution unlimited.		18a. DECLASSIFICATION/DOWNGRADING SCHEDULE
17. DISTRIBUTION STATEMENT (of the abstract entered in Block 20, if different from Report)		
18. SUPPLEMENTARY NOTES		
19. KEY WORDS (Continue on reverse side if necessary and identify by block number) Fluid dynamics, numerical simulation, viscid flow		
20. ABSTRACT (Continue on reverse side if necessary and identify by block number) (hmn) This paper describes the application of a semidirect method to the calculation of the flow near a sliding corner. On a set of successively refined grids the Navier-Stokes equations modeling the steady state viscous, incompressible, low Reynolds number flow are solved in terms of the vorticity and stream function in Cartesian coordinates for a slab geometry. The calculated flow field allows preliminary estimate of the nature of the flow at the sliding corner.		

DD FORM 1 JAN 73 1473

EDITION OF 1 NOV 65 IS OBSOLETE

UNCLASSIFIED

SECURITY CLASSIFICATION OF THIS PAGE (When Data Entered)

TABLE OF CONTENTS

	Page
I. INTRODUCTION.	5
II. THE MODEL PROBLEM	5
III. THE BOUNDARY CONDITIONS	6
IV. THE ALGORITHM	7
V. THE CALCULATIONAL SETUP	7
VI. DESCRIPTION OF RESULTS.	8
VII. CONCLUSIONS AND OUTLOOK	9
DISTRIBUTION LIST	19

DTIC
ELECTE
S JUN 3 1980 D
B

ACCESSION for		
NTIS	White Section	<input checked="" type="checkbox"/>
DDC	Buff Section	<input type="checkbox"/>
UNANNOUNCED		<input type="checkbox"/>
JUSTIFICATION _____		
BY _____		
DISTRIBUTION/AVAILABILITY CODES		
Dist.	AVAIL. and/or	SPECIAL
A		

I. INTRODUCTION

One of the vexing problems in the implementation of multidimensional computer codes for interior ballistics applications is the proper handling of the flow singularity at the conjunction of the gun tube wall and the base of a moving projectile. The value of an incorrectly determined flow variable at this point is likely to be propagated into the interior of the flow, possibly leading to disastrous consequences for the rest of the flow field. In the past, the corner point singularity was treated by ignoring it, i.e., using a coarse mesh with a computational stencil which does not include the corner point, or by assuring that the corner is multivalued, i.e., it is both at rest and moving with the projectile velocity. Neither of these approaches is completely satisfactory. The nature of the flow immediately adjacent to the corner should suggest the correct boundary condition at the corner point itself. Consequently, we apply a computational stencil which excludes the corner point and examine the nature of and changes in the flow field as we approach the sliding corner point by a series of grid refinements.

II. THE MODEL PROBLEM

Consider a smooth bore gun tube at an early time in the ballistic cycle. The projectile, propelled by the high pressure combustion gases, proceeds down the gun tube. For the case at hand, the obturation is perfect, blowby is not allowed. The flow field behind the accelerating projectile consists of a core flow, boundary layers on the gun tube walls and projectile base, and the corner flow.

Looking at a slab cut out of this tube along any diameter, we have abstracted the following configuration: a rectangular region bounded on the right by a moving projectile, below by a smooth adiabatic impermeable wall, above by the axis of symmetry and at the left by the inflowing gas with a given velocity distribution.

The flow is assumed to be incompressible, viscid and steady throughout the region of interest. From the Navier-Stokes equations, and the definition of vorticity

$$\zeta = \frac{\partial u}{\partial y} - \frac{\partial v}{\partial x} \quad (1)$$

one obtains the vorticity transport equation

$$\frac{\partial \zeta}{\partial t} = -u \frac{\partial \zeta}{\partial x} - v \frac{\partial \zeta}{\partial y} + \nu \frac{\partial^2 \zeta}{\partial x^2} + \frac{\partial^2 \zeta}{\partial y^2} \quad (2)$$

With the definition of the stream function

$$\frac{\partial \psi}{\partial y} = u, \quad \frac{\partial \psi}{\partial x} = -v \quad (3)$$

equation (1) transforms into the Poisson equation

$$\nabla^2 \psi = \zeta \quad (4)$$

Introducing a characteristic length, L , the tube radius, and a time defined as the advective time constant (L/\bar{u}_0), with \bar{u}_0 a characteristic constant projectile speed, the equation may be brought into the following nondimensional form

$$\zeta_t = -Re \nabla \cdot (\underline{v} \zeta) + \nabla^2 \zeta \quad (5)$$

and

$$\nabla^2 \psi = \zeta \quad (6)$$

where ζ is the vorticity nondimensionalized by (\bar{u}_0/L), Re is the Reynolds number, \underline{v} the vector velocity. Subscripts denote partial differentiation. Since we are looking at the steady case only, $\zeta_t = 0$. A moving coordinate system is now introduced which brings the projectile to rest. One of the advantages which accrues is that one does not have to deal with partial cells in the course of the calculation.

III. THE BOUNDARY CONDITIONS

Along the inflow boundary, Poiseuille flow and thus the values of the stream and vorticity functions are specified. The upper boundary is the axis of the tube, a line of symmetry at which $\zeta = 0$ and ψ is determined from $u_{\max} = \frac{\partial \psi}{\partial y}$.

In the projectile fixed coordinate system the lower boundary moves to the left at a velocity of $u = -1$ and ψ , the stream function, is set equal to zero. The wall vorticity ζ_w is calculated from Woods' equation; see reference 1 for details. The basic idea is to expand the stream

1. Roache, P.J., Computational Fluid Dynamics, Revised Printing, Hermosa Publishers, Albuquerque, New Mexico, 1976.

function in a Taylor series around a point one mesh width away from the wall retaining terms up to the third order. Using the definition of vorticity and applying the no slip condition on the surface one arrives at

$$\zeta_w = \frac{3(\psi_{w+1} - \psi_w)}{\Delta y^2} - \frac{1}{2}\zeta_{w+1}$$

where the subscripts $w+1$ and w denote a point one mesh width away from the wall and the wall point, respectively. A similar expression holds along the piston face.

The boundary conditions on the projectile were as follows: points along the projectile base have zero velocity components; thus the stream function is zero.

IV. THE ALGORITHM

A semidirect solution technique was used, motivated by the efficiency of these methods. As in (2), the equations are first linearized, then solved directly; subsequently the linearization is updated and the iteration is repeated. Unlike the method in (1), the variable coefficient advection terms are included in the direct linear solution by the use of marching methods (3).

The marching method is unstable for elliptic partial differential equations as the mesh is refined, i.e., as $\Delta l \rightarrow 0$ where Δl is the mesh size. For finite mesh widths, however, usable results may be obtained.

Converged answers are typically obtained in less than 10 iterations. The total computational time on a CDC 6600 is of the order of 5-10 msec/cell. No empirical or semi-empirical factors (such as time steps, under-relaxation factors, etc.) need to be determined.

V. THE CALCULATIONAL SETUP

In a planar geometry, a series of calculations were carried out with the number of grid points varying from 11×11 to 41×41 . While the radial dimension was one in all cases, the axial dimension was increased from 1, as the number of cells were increased, such that the cell aspect ratio, axial to radial dimension varied from 1:1 to 4:1.

2. Roache, P.J., and Ellis, M.A., "The BID Method for the Steady-State Navier-Stokes Equations", Computers and Fluids, 3, 305-320 (1975).
3. Roache, P.J., "Marching Methods for Elliptic Problems: Part 1," Numerical Heat Transfer 1, 1-25 (1978). "Part 2", 1, 163-181 (1978).

It was unfortunate that stability requirements of the algorithm necessitated the use of these cell aspect ratios which made direct comparison among the several runs difficult. In all cases the wall was accelerated to the left at a velocity of -1. A very gentle pressure gradient, of the order of 1%, was imposed in the axial direction.

To start the calculation, an upstream Poiseuille flow profile, of the form $\psi = y - 1.5y^2 + 0.5y^3$, where ψ is the stream function and y the radial distance, was prescribed. Analogous prescriptions were made for the vorticity. To initialize, the Reynolds number was set to zero, then in increments of 10 it was raised to 50 in the course of the calculation for a given computational mesh.

Several checks monitored the progress of the calculation. If the calculation failed to converge in 21 iterations, the calculation was broken off, and an error message printed. In addition, the results of two convergence checks were printed out.

VI. DESCRIPTION OF THE RESULTS

Based on experimental observations and classical analysis, one expects the Poiseuille flow to persist in the tube coupled with a region of intense vortex generation at the corner itself. This expectation was borne out by the numerical calculations which we now proceed to describe.

The results are best illustrated in terms of plots of the flow variables. The first figure shows the velocity profile at the position 0.6 from the upstream (inflow) boundary for $Re = 30$. It is a Poiseuille profile in the transformed coordinates.

Next the contour plot of the u velocity component gives an idea of the gradients in the flow velocity in the computational regime. The contour lines are spaced at 0.2. An even better overall view can be obtained from the vector velocity plot, Figure 3. Note that the flow (in the projectile fixed coordinates) is parallel to the tube axis, then along the face of the projectile, finally turning around and exiting. Since it is incompressible, the flow in and out of the region of interest must balance exactly.

A significant insight into the nature of the flow singularity in the corner, of course, is furnished by the vorticity plots, Figures 4-7. The contour lines are spaced at 2.0. While the contour plot gives a good overall idea of the vorticity distribution, more detail is furnished by vorticity plotted along the wall as well as vorticity along the projectile face.

In both instances we see that near the corner singularity the vorticity rises sharply. This is readily seen in the three-dimensional plot, Figure 7. Also, as the calculations showed, the level of vorticity is increased minimally as the Reynolds number was raised from 10 to 50, but by up to 20% in going to a 31×31 mesh from an 11×11 (see Figures 6 and 8). Away from the corner in the axial direction, practically there was no variation in the level as is evident in Figure 6, for example.

The results further show that the lower wall is contributing the major share of the vorticity generation. Indeed, if one considers the ratio of the vorticity generated by the lower wall to that generated along the projectile base, say one mesh width away from the corner, for a mesh of 31×31 at $Re = 10$ the ratio is 1.8. Similar ratios are obtained for the other calculated meshes.

The coarseness of the mesh, as well as the cell aspect ratio, had a definite effect on the maximum level of vorticity. As the number of cells was increased, the cells were also stretched; the resulting mesh refinement moved the cell centers further away from the corner in the axial direction.

One should note, however, that these results must be interpreted carefully, since in these preliminary runs mesh independence of the vorticity was not obtained.

VII. CONCLUSIONS AND OUTLOOK

At this point our conclusions are preliminary in nature. We found, through mesh refinement near the confluence of the projectile and a moving wall, that the calculated flow there conforms to qualitative estimates.

As one proceeds radially from the corner, the velocity, in the transformed coordinates, is seen to decrease. This is true in the neighborhood of the sector formed by the projectile and the cylinder wall.

The vorticity function exhibits a sharp rise as one approaches the corner along the wall in the axial direction, and a sharp drop when the approach is from the radial direction, reminding one of a sink type flow behavior.

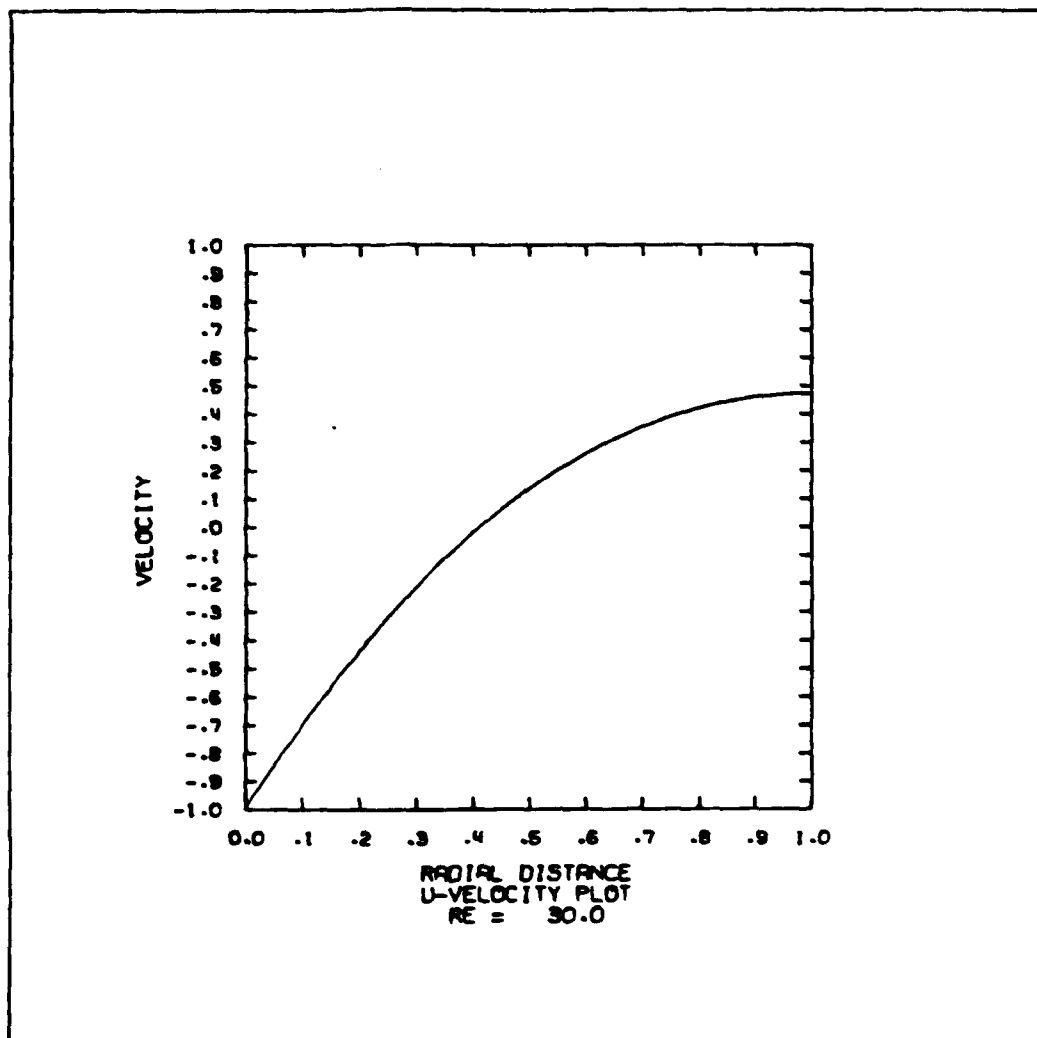


Figure 1. Velocity Profile at a Position 0.6 from the Inflow Boundary at $Re=30$.

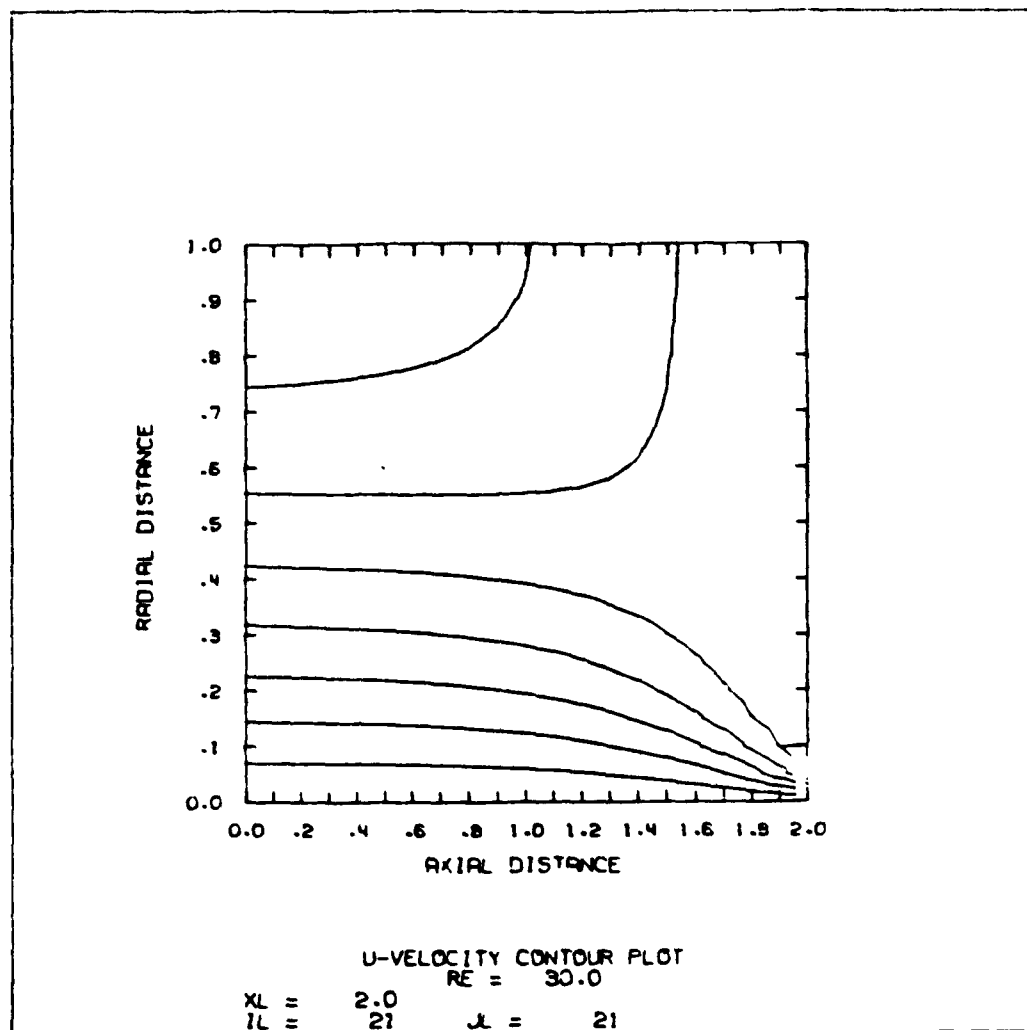


Figure 2. Contour Plots of the Axial Velocity Component in the Computational Region.

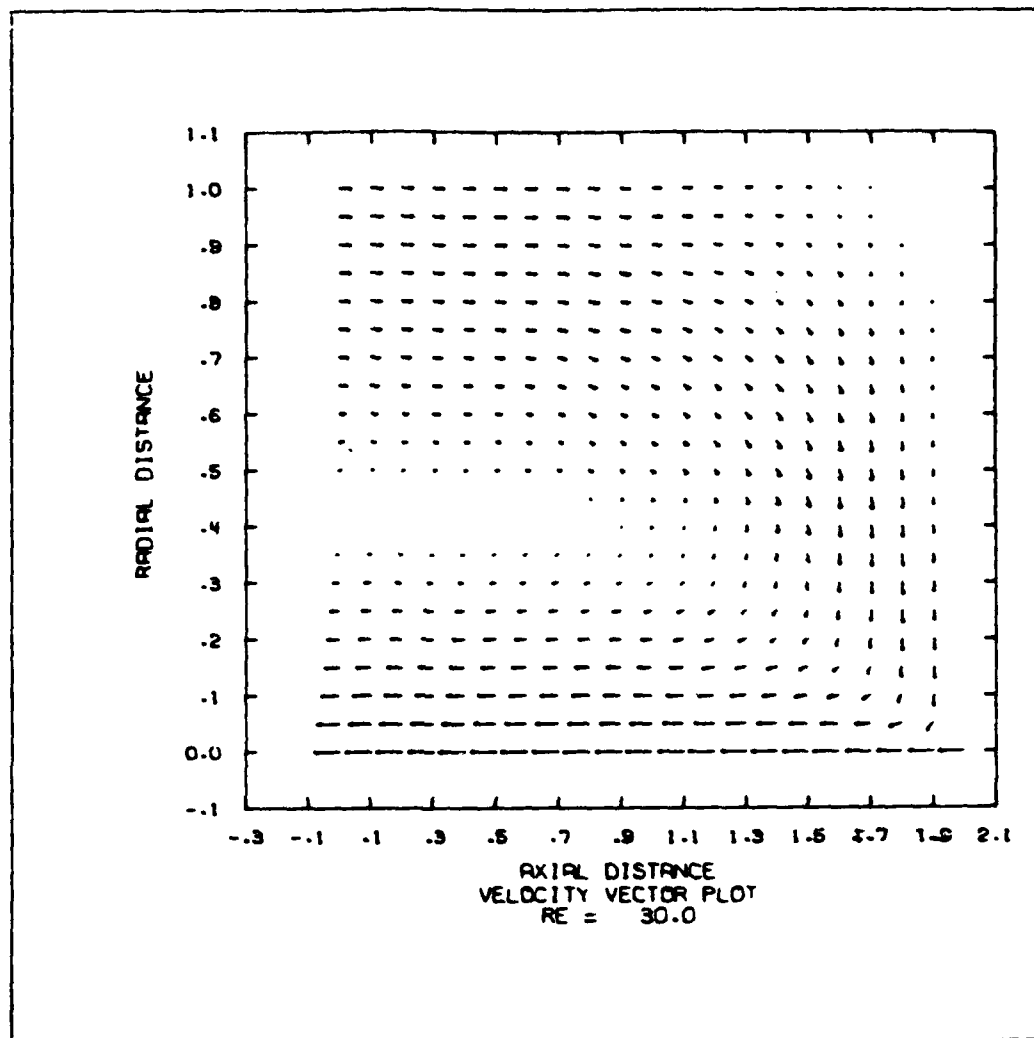


Figure 3. Vector Velocity Plot.

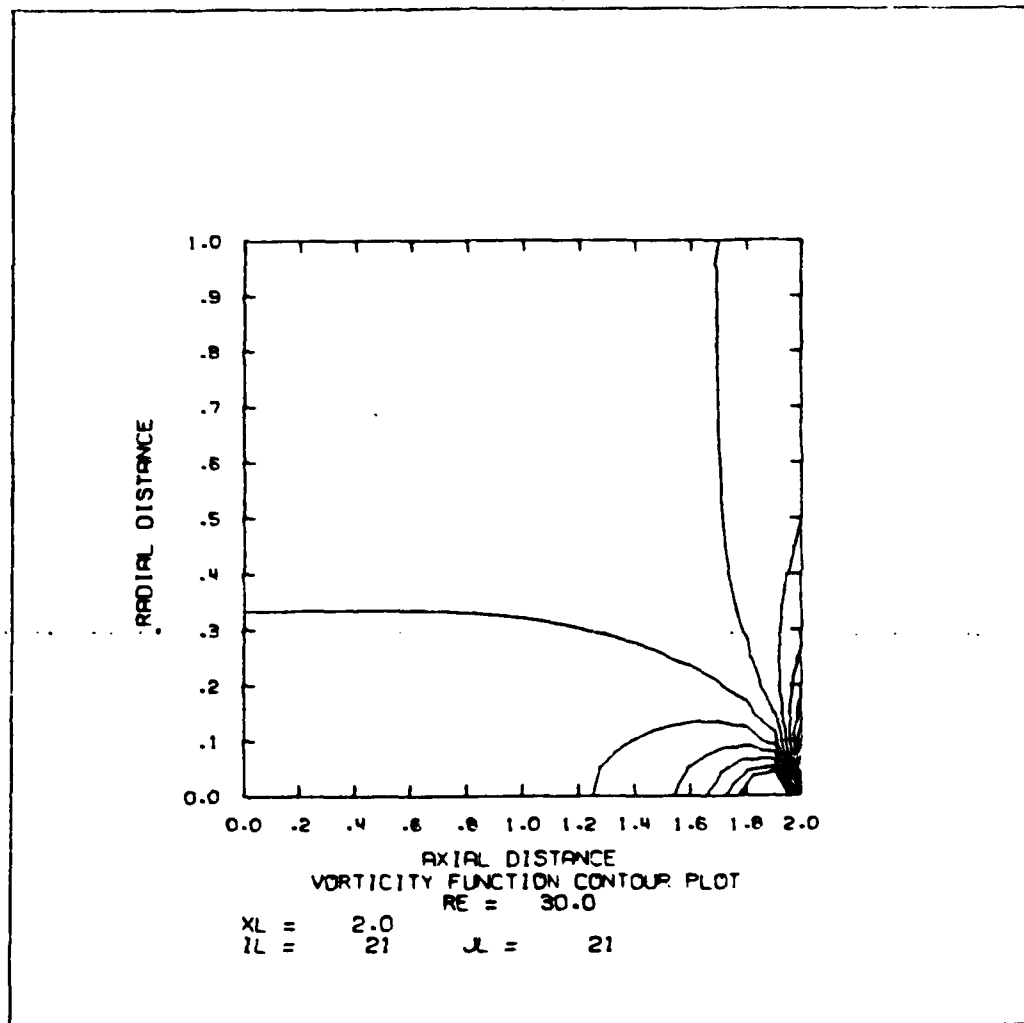


Figure 4. Vorticity Function Contour Plot at $Re=30$.

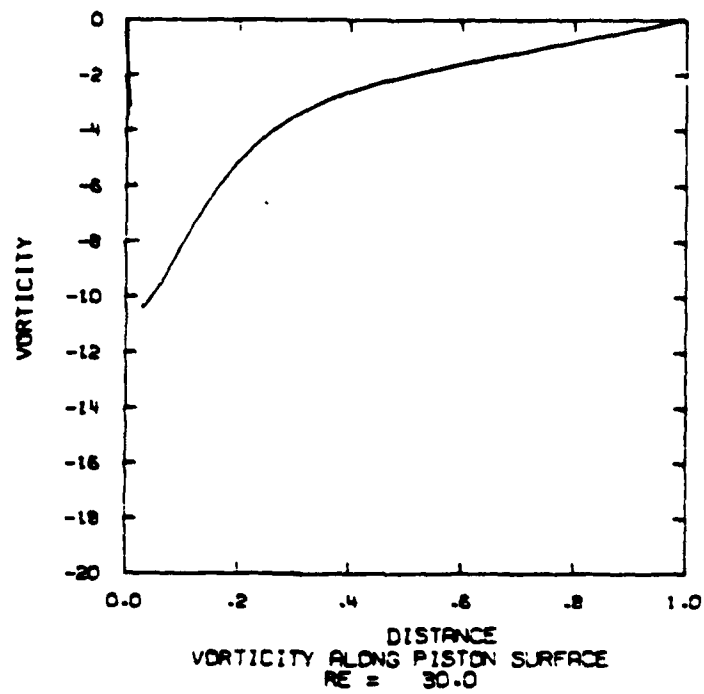


Figure 5. Vorticity Along the Piston Surface.

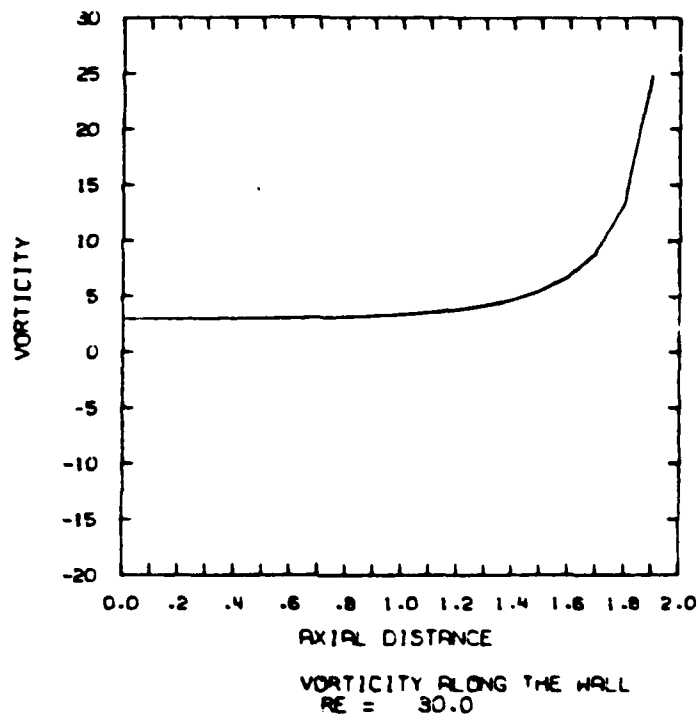


Figure 6. Vorticity Along the Lower Wall.

VORTICITY

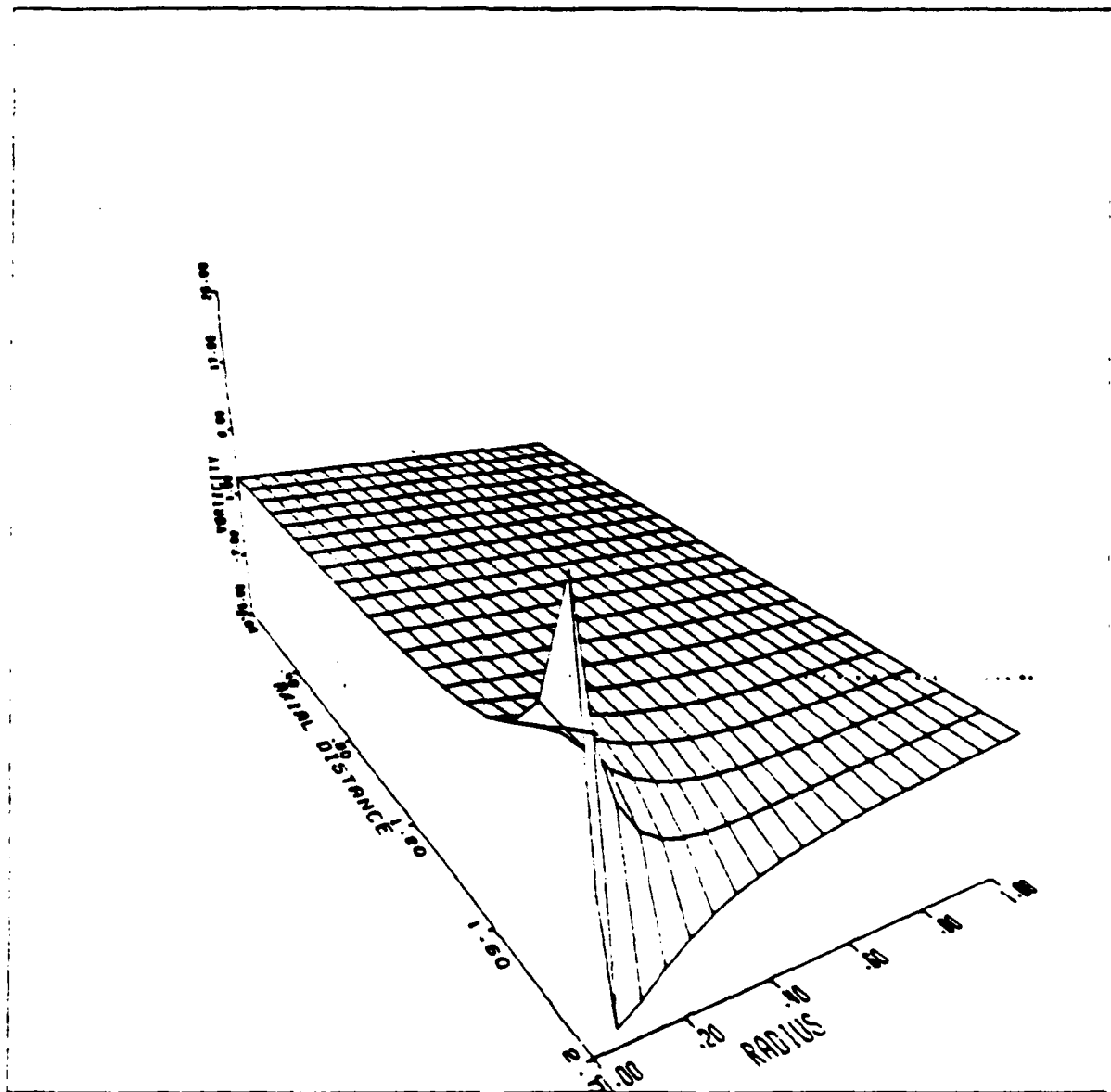


Figure 7: Vorticity Surface Plot in the Computational Domain.

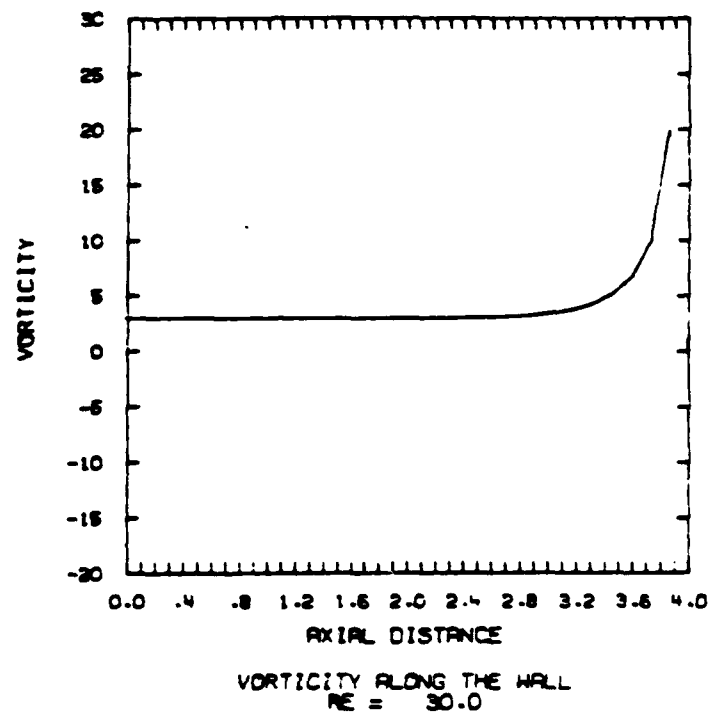


Figure 8. Vorticity Along the Wall for Coarser Mesh Definition.

DISTRIBUTION LIST

<u>No. of Copies</u>	<u>Organization</u>	<u>No. of Copies</u>	<u>Organization</u>
12	Commander Defense Technical Info Center ATTN: DDC-DDA Cameron Station Alexandria, VA 22314	1	Commander US Army Communications Rsch and Development Command ATTN: DRDCO-PPA-SA Fort Monmouth, NJ 07703
1	Commander US Army Materiel Development and Readiness Command ATTN: DRCDMD-ST 5001 Eisenhower Avenue Alexandria, VA 22333	1	Commander US Army Electronics Research and Development Command Technical Support Activity ATTN: DELSD-L Fort Monmouth, NJ 07703
2	Commander US Army Armament Research and Development Command ATTN: DRDAR-TSS (2 cys) Dover, NJ 07801	2	Commander US Army Missile Command ATTN: DRDMI-R DRDMI-YDL Redstone Arsenal, AL 35809
1	Commander US Army Armament Materiel Readiness Command ATTN: DRSAR-LEP-L, Tech Lib Rock Island, IL 61299	1	Commander US Army Tank Automotive Rsch and Development Command ATTN: DRDTA-UL Warren, MI 48090
1	Director US Army ARRADCOM Benet Weapons Laboratory ATTN: DRDAR-LCB-TL Watervliet, NY 12189	1	Director US Army TRADOC Systems Analysis Activity ATTN: ATAA-SL, Tech Lib White Sands Missile Range NM 88002
1	Commander US Army Aviation Research and Development Command ATTN: DRSAB-E P.O. Box 209 St. Louis, MO 61366	1	SRA ATTN: Mr. H. McDonald P.O. Box 498 Glastonbury, CT 06033
1	Director US Army Air Mobility Research and Development Laboratory Ames Research Center Moffett Field, CA 94035	1	Ecodynamics Research Associates ATTN: Dr. P.J. Roache P.O. Box 8172 Albuquerque, NM 87108

DISTRIBUTION LIST

<u>No. of Copies</u>	<u>Organization</u>
1	Los Alamos Scientific Laboratory ATTN: C.L. Mader P.O. Box 1663 Los Alamos, NM 87545

Aberdeen Proving Ground

Dir, USAMSAA
ATTN: DRXSY-D
DRXSY-MP, H. Cohen
Cdr, USATECOM
ATTN: DRSTE-TO-F
Dir, Wpns Sys Concepts Team,
Bldg E3516, EA
ATTN: DRDAR-ACW

USER EVALUATION OF REPORT

Please take a few minutes to answer the questions below; tear out this sheet and return it to Director, US Army Ballistic Research Laboratory, ARRADCOM, ATTN: DRDAR-TSB, Aberdeen Proving Ground, Maryland 21005. Your comments will provide us with information for improving future reports.

1. BRL Report Number _____

2. Does this report satisfy a need? (Comment on purpose, related project, or other area of interest for which report will be used.)

3. How, specifically, is the report being used? (Information source, design data or procedure, management procedure, source of ideas, etc.)

4. Has the information in this report led to any quantitative savings as far as man-hours/contract dollars saved, operating costs avoided, efficiencies achieved, etc.? If so, please elaborate.

5. General Comments (Indicate what you think should be changed to make this report and future reports of this type more responsive to your needs, more usable, improve readability, etc.)

6. If you would like to be contacted by the personnel who prepared this report to raise specific questions or discuss the topic, please fill in the following information.

Name: _____

Telephone Number: _____

Organization Address: _____

